

# Nanocapsules for self-healing materials

B.J. Blaiszik<sup>a</sup>, N.R. Sottos<sup>b,d,\*</sup>, S.R. White<sup>c,d</sup>

<sup>a</sup> *Theoretical and Applied Mechanics Program – Mechanical Science and Engineering Department, University of Illinois at Urbana-Champaign, Urbana, IL 61801, United States*

<sup>b</sup> *Department of Materials Science and Engineering, University of Illinois at Urbana-Champaign, Urbana, IL 61801, United States*

<sup>c</sup> *Department of Aerospace Engineering, University of Illinois at Urbana-Champaign, Urbana, IL 61801, United States*

<sup>d</sup> *Beckman Institute for Advanced Science and Technology, University of Illinois at Urbana-Champaign, Urbana, IL 61801, United States*

Received 10 April 2007; received in revised form 25 July 2007; accepted 26 July 2007

Available online 8 August 2007

## Abstract

We report an *in situ* encapsulation method demonstrating over an order of magnitude size reduction for the preparation of urea–formaldehyde (UF) capsules filled with a healing agent, dicyclopentadiene (DCPD). Capsules with diameters as small as 220 nm are achieved using sonication techniques and an ultrahydrophobe to stabilize the DCPD droplets. The capsules possess a uniform UF shell wall (77 nm average thickness) and display good thermal stability. By controlling the  $\zeta$ -potential, the capsules are uniformly dispersed in an epoxy matrix and shown to cleave rather than debond upon fracture of the matrix. Mechanical properties of the epoxy/capsule composite, including mode-I fracture toughness, elastic modulus, and ultimate tensile strength are measured and compared to previous data for larger capsules (ca. 180  $\mu\text{m}$ ).

© 2007 Elsevier Ltd. All rights reserved.

**Keywords:** A. Nanostructures; A. Smart materials; A. Polymer–matrix composites; B. Mechanical properties; Self-healing materials

## 1. Introduction

Damage in polymeric coatings, adhesives, microelectronic components, and structural composites can span many length scales. Structural composites subject to impact loading can sustain significant damage on the order of tens of centimeters, which in turn can lead to subsurface millimeter scale delaminations and micron scale matrix cracking. Coatings and microelectronic packaging components have cracks that initiate on even smaller length scales. Repair of large-scale damage (e.g. a projectile or blast impact) is difficult and, when possible, requires use of bonded composite patches over the effective area. For

smaller scale crack damage, however, a novel method of autonomic repair has been achieved through the use of self-healing polymers [1].

Crack healing is accomplished by dispersing capsules containing a healing agent and a solid catalyst within a polymer matrix. Damage in the form of a crack serves as the triggering mechanism for self-healing as injury does in biological systems. The approaching crack ruptures the embedded microcapsules, releasing healing agent into the crack plane through capillary action. Polymerization of the healing agent is initiated by contact with the embedded catalyst, bonding the crack faces.

Self-healing polymers and composites that incorporate microencapsulated healing agents have demonstrated high levels of healing efficiency in both static and dynamic loading conditions [2–4]. Microcapsules that contain the healing agent must possess adequate strength, long shelf-life, and excellent bonding to the host material. In previous work we have shown that

\* Corresponding author. Address: Theoretical and Applied Mechanics Program – Mechanical Science and Engineering Department, University of Illinois at Urbana-Champaign, Urbana, IL 61801, United States. Tel.: +1 217 244 0052.

E-mail address: [n-sottos@uiuc.edu](mailto:n-sottos@uiuc.edu) (N.R. Sottos).

urea–formaldehyde capsules containing dicyclopentadiene (DCPD) prepared by *in situ* polymerization in an oil-in-water emulsion meet these requirements for self-healing epoxy [5]. However, standard emulsion encapsulation procedures reach a lower limit of approximately 10  $\mu\text{m}$  in capsule diameter. In the current work, we demonstrate over an order of magnitude reduction in size scale by a combination of ultrasonication and *in situ* encapsulation techniques. Development of submicron capsules and nanocapsules filled with healing agent will allow for the incorporation of healing functionality in composites with interstitial spacing smaller than capsules prepared using previous methods.

Submicron capsules and particles have been prepared previously for encapsulation of inorganic particles such as magnetite in polystyrene [6], pressure sensitive adhesives [7], and melamine-formaldehyde capsules containing cyclohexane and *n*-octadecane [8]. An emulsion stabilized by an ultrahydrophobe in the presence of high shear induced by ultrasonic processing leads to the formation of submicron droplets of oil in water [9,10]. The process of *in situ* polymerization has been used to produce microcapsules as described in the previous works of Brown et al. [5], Ni et al. [7], and Alexandridou et al. [11]. The current work extends *in situ* polymerization studies of UF encapsulation of DCPD to submicron size scales utilizing costabilization techniques described in the mini-emulsion literature [12,13].

The addition of particulate fillers, such as capsules, to an epoxy resin can have a significant influence on the mechanical properties of a material. Particle fillers can lead to fracture toughness increases by multiple phenomena including, but not limited to, crack pinning [14], crack bridging [15], microcracking [16], and crack deflection [17,18]. In each case, the properties of the toughening filler, the filler volume fraction, and filler to matrix adhesion are important parameters in determining the level of toughening. Examples of particle induced toughening in thermoset resins have been reported for hollow glass cenospheres [19], silica

nanoparticles [20,21], multi-layered rubbery nanoparticles [22], and for  $\text{Al}_2\text{O}_3$  nanocomposites [23]. Brown et al. [2,24] reported significant increases in fracture toughness of a DGEBA epoxy matrix with varying concentrations of DCPD filled microcapsules ranging in diameter from 50  $\mu\text{m}$  to 460  $\mu\text{m}$ .

In addition to fracture toughness, microcapsules affect the elastic modulus of the composite. For example, an increase in elastic modulus was observed when glass cenospheres were added to a polyester matrix [19]. However, decreasing elastic modulus [25,26] and ultimate tensile strength [26] has been reported with increasing concentration of UF capsule concentration of relatively large (ca. 180  $\mu\text{m}$ ) capsules. In this study, we measure the fracture toughness, elastic modulus, and tensile properties of epoxy composites with UF capsules (ca. 1.5  $\mu\text{m}$ ) and compare these results with previous studies by Brown et al. using larger UF capsules.

## 2. Materials and methods

### 2.1. Capsule preparation

Submicron capsules containing DCPD monomer were prepared by *in situ* polymerization of urea and formaldehyde using a modified process of Brown et al. [5], which is summarized in Fig. 1a. DCPD (15.5% w/v) was slowly added to 30 ml of a room temperature solution of 1.5% ethylene-maleic anhydride copolymer (Zemac-400 EMA), urea, resorcinol, and ammonium chloride and allowed to equilibrate under stirring conditions for 10 min before sonication. For some capsule batches, an ultrahydrophobe, either hexadecane or octane, was added to the DCPD as a costabilizer to increase the hydrophobicity of the inner phase and decrease Ostwald ripening [10]. The tapered 3.2 mm tip sonication horn of a 750 W ultrasonic homogenizer (Cole-Parmer) was placed in the solution, as shown in Fig. 1b, for 3 min at 40% intensity ( $\sim 3.0$  kJ of input energy) with continuous mixing at 800 rpm. This sonica-

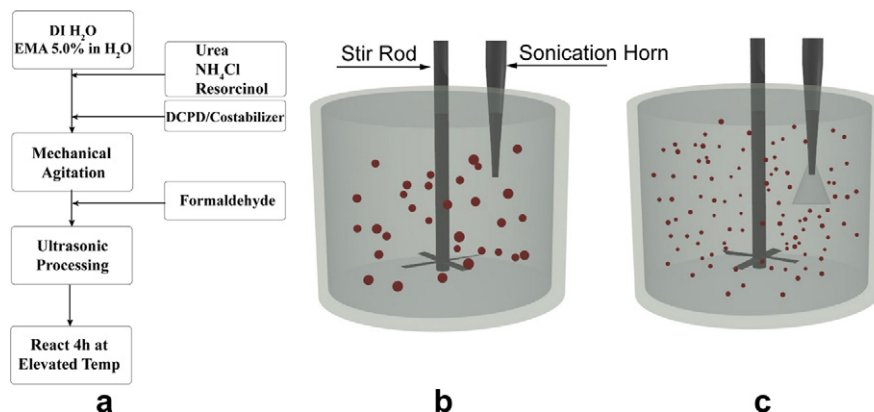


Fig. 1. Encapsulation method for preparing UF capsules containing DCPD using sonication: (a) process flow chart; (b) schematic showing the emulsion prior to sonication and (c) during sonication.

tion step changes the emulsion from slightly cloudy to opaque white. Formalin (37% formaldehyde) was then added in the same ratio as described previously by Brown et al. [5]. The temperature control bath was slowly heated and held constant for 4 h of reaction. At the completion of the reaction, the mechanical agitation and heating were stopped, and the pH was adjusted to 3.50 with sodium hydroxide.

## 2.2. Capsule dispersion in epoxy

Capsules filled with the healing agent DCPD were cooled in an ice bath to ensure dispersion stability. Anhydrous magnesium sulfate, a drying agent, was added to the aqueous capsule solution and the capsules were washed with a solvent to remove excess EMA surfactant. The resulting solution was centrifuged to separate the capsules from the solution. Multiple washes and centrifugation steps were necessary to remove excess water and surfactant. The resulting capsule mass was allowed to air dry between 0 and 30 min before it was mixed into the epoxy. The optimal air dry time appeared to be between 10 and 15 min at ambient conditions. Capsules were then dispersed using ultrasonication and high speed stirring in an epoxy matrix of EPON 828 (DGEBA) resin cured with Ancamine (DETA). Homogeneous capsule dispersion in epoxy was highly dependent on capsule dry time, capsule size, epoxy sonication time, separation method, and various capsule preparation parameters.

For mechanical testing and shell wall analysis, capsules were dispersed in EPON 828 resin as described above, mixed with 12 pph DETA curing agent, and molded into the desired specimen shape. Fracture toughness was measured using a tapered double cantilever beam (TDCB) sample (Fig. 2a) [2,27], tensile strength was measured using the sample shown in Fig. 2b, and the elastic modulus was measured using prismatic rectangular bars ( $h = 1.5$  mm,  $w = 1.0$  mm,  $l = 15.0$  mm) prepared for dynamic mechanical analysis (DMA). For measurement of shell wall thickness, cylindrical epoxy samples ( $d = 8.0$  mm,  $h =$

16.0 mm) were frozen in liquid nitrogen and fractured with a razor blade. Each specimen was subjected to the same curing conditions of 24 h at room temperature followed by 24 h in an oven at 35 °C immediately prior to testing.

## 3. Microcapsule characterization

A series of characterization tests were carried out on the capsules prior to embedding in the epoxy matrix to assess capsule morphology, physical properties and stability. Shell wall integrity, aggregation phenomena, and microcapsule size were observed by scanning electron microscopy (SEM). Capsule samples were prepared on glass slides, dried in a vacuum oven, and sputter coated with gold-palladium. The SEM measurements were made at 5.0 kV accelerating voltage with a spot size of 3.0 to minimize sample charging. The SEM images revealed that the capsules were spherical in shape, nearly monodisperse in capsule diameter, and had a smooth non-porous shell wall. The capsule shell walls were free of the thick layer of UF debris seen by Brown et al. in previous studies [5]. SEM was also used to investigate clumping problems caused by insufficient surfactant concentration. Fig. 3a shows a characteristic clump of capsules which results when the concentration of EMA surfactant for capsule formation was too low. The optimized EMA concentration was found using a binary search with the criterion of minimizing EMA concentration without clump formation. Capsule clumps formed with low concentrations of EMA were inseparable by ultrasonication, stirring, and solvent washing. Capsules shown in Fig. 3b were processed using the optimized capsule preparation process and were dispersible in epoxy.

### 3.1. Capsule size analysis

Capsule size analysis was performed by two different methods, SEM and focused extinction (PSS Accusizer FX). A characteristic focused extinction histogram for capsules without costabilizer is shown in Fig. 4a. Focused extinction mean values were calculated from over 50,000 measurements and SEM mean values were calculated from a minimum of 200 individual measurements obtained from photomicrographs. The capsules prepared with a core material of pure DCPD had a mean diameter of  $1.56 \pm 0.50$   $\mu\text{m}$  measured by focused extinction and  $1.65 \pm 0.79$   $\mu\text{m}$  via SEM measurements.

Capsule size was further reduced by the addition of costabilizer to minimize Ostwald ripening. The effect of costabilizer on the final capsule diameter is summarized in Fig. 4b for 0–10 wt% hexadecane and 0–30 wt% octane, and listed numerically in Table 1. The smallest batch of capsules, had a mean diameter of  $220 \pm 113$  nm measured by SEM, and was achieved with 10 wt% hexadecane costabilizer. Images of the nanocapsules show spherical capsules, free of surface debris (Fig. 5a) with well formed shell walls (Fig. 5b).

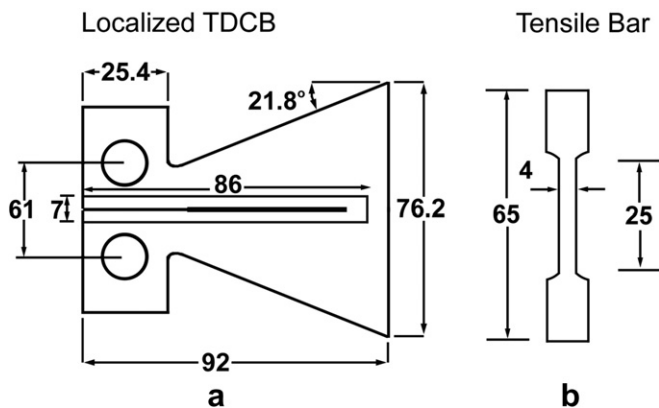


Fig. 2. Test samples used to measure (a) mode-I fracture toughness and (b) tensile strength. All specimen dimensions are given in millimeters.

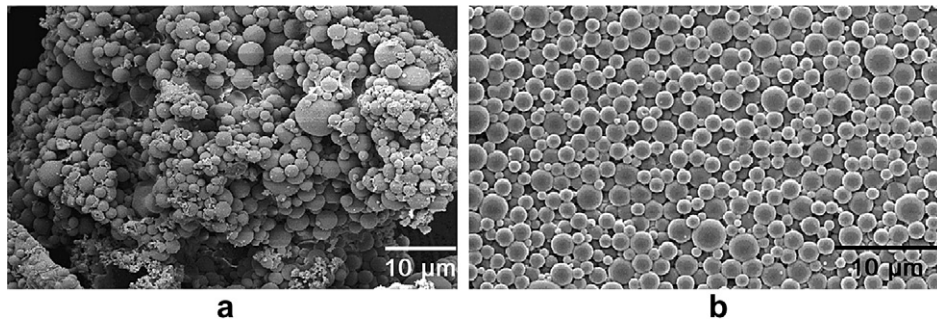


Fig. 3. (a) Aggregated capsules prepared using a low concentration of the surfactant EMA and (b) separated capsules produced using optimized concentration of the surfactant EMA.

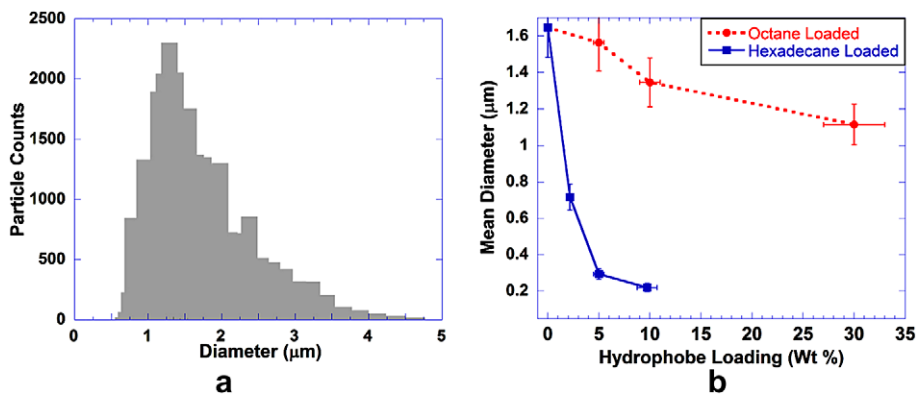


Fig. 4. (a) Size distribution of microcapsules prepared using sonication technique as measured by focused extinction, (b) mean capsule diameter for different ratios of DCPD to costabilizer: octane (●) and hexadecane (■).

Table 1  
Capsule characterization results

Conditions	Diameter (μm)	Wall thickness (nm)	DCPD Mass (%)	Fill (%)
Standard capsules (550 RPM stirring) <sup>a</sup>	183 ± 42	190 ± 30	79–92	–
Sonicated capsules	1.56 ± 0.50	77 ± 25 <sup>b</sup>	78.4	94
Sonicated capsules	1.65 ± 0.79 <sup>b</sup>	–	–	–
Sonicated capsules (2% hexadecane)	0.717 ± 0.32	–	–	–
Sonicated capsules(5% hexadecane)	0.294 ± 0.15	–	–	–
Sonicated capsules(10% hexadecane)	0.220 ± 0.11 <sup>b</sup>	20 ± 3 <sup>c</sup>	–	–

<sup>a</sup> Brown et al. [4].

<sup>b</sup> SEM measurement.

<sup>c</sup> TEM measurement.

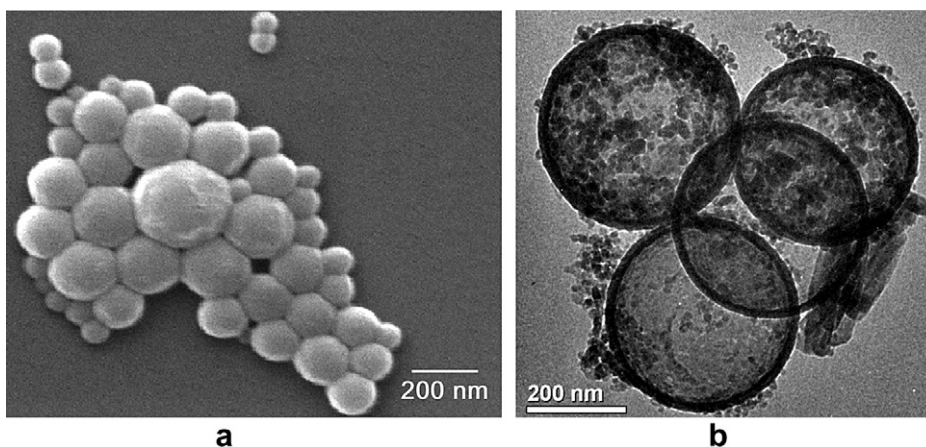


Fig. 5. (a) SEM images of nanocapsules produced with hexadecane costabilizer and (b) TEM images showing the core-shell morphology of the produced nanocapsules.

### 3.2. Shell wall thickness

Shell wall thickness was measured directly from SEM images of the fracture surfaces for capsules containing DCPD without costabilizer (ca. 1.5  $\mu\text{m}$  diameter). Measurements were collected from two independent batches using ImageJ image analysis software. The combined data set is presented in Fig. 6. The mean shell wall thickness was  $77 \pm 25$  nm. For the smallest capsules produced (ca. 200 nm diameter), shell wall thickness was estimated as  $20 \pm 3$  nm from TEM images (Fig. 5b). Previous studies of larger UF microcapsules reported a substantially thicker shell wall of  $190 \pm 30$  nm [5,25].

### 3.3. Thermal stability of capsules

Thermal stability and overall quality of the prepared capsules was assessed by thermogravimetric analysis (TGA) at a heating rate of  $10$   $^{\circ}\text{C}/\text{min}$ . Capsule samples were allowed to dry at  $80$   $^{\circ}\text{C}$  for 2 h before thermal testing to remove residual water. In Fig. 7, a representative TGA trace for optimized capsules with a stable shell wall is compared to that for leaky capsules with lower DCPD content. The TGA performed on capsules prepared using the optimized processing method showed less than 5% capsule weight loss before  $100$   $^{\circ}\text{C}$  (i.e. residual water). In addition, a sharp drop in weight percent occurred from  $150$  to  $220$   $^{\circ}\text{C}$ . This drop corresponded closely to the boiling point of DCPD ( $170$   $^{\circ}\text{C}$ ), and indicated that the capsules were stable up to the rupture and release of the vaporized healing agent.

### 3.4. Capsule fill content analysis

The fill content of the capsules was examined by gas chromatography to determine the presence of DCPD in the processed capsules. Prior to testing the composition

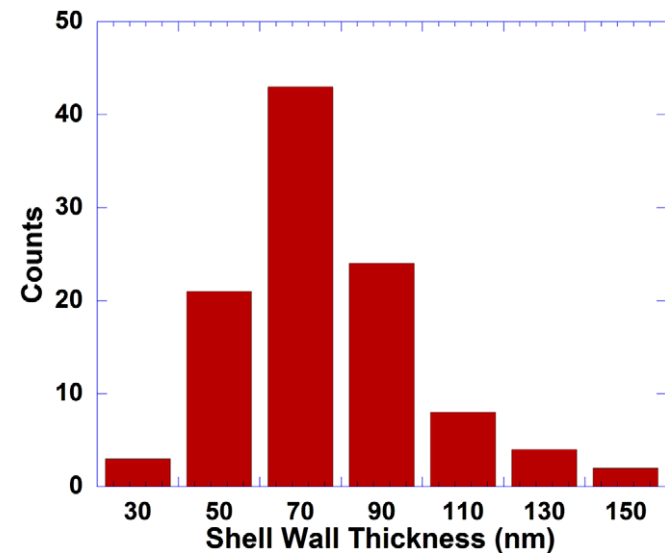


Fig. 6. Distribution of the shell wall thickness of capsules prepared without costabilizer as measured by SEM. This data was collected from two independent sample batches and includes 106 individual measurements.

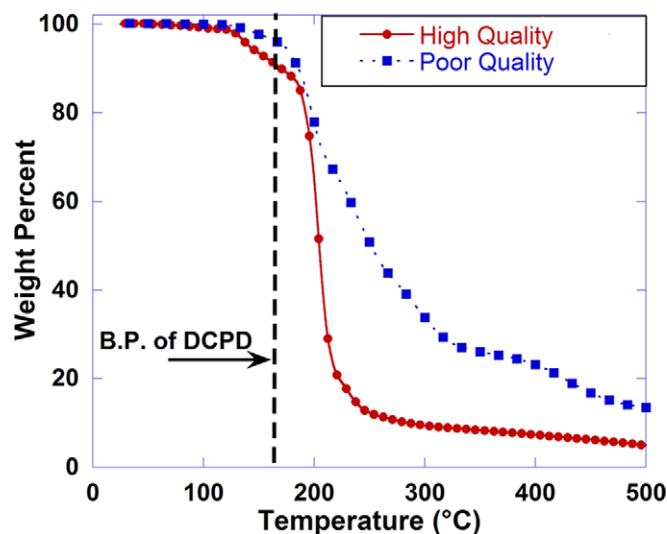


Fig. 7. Characteristic TGA traces for dried  $1.5$   $\mu\text{m}$  mean diameter capsules prepared using sonication technique. High quality capsules show a rupture event and significant weight loss near the boiling point of DCPD. Low quality capsules show more gradual weight loss in this regime and a greater percentage of retained weight above  $300$   $^{\circ}\text{C}$  associated with the decomposition of the urea–formaldehyde shell wall.

of the capsules, authentic traces of methylene chloride, endo-DCPD, and exo-DCPD were used to determine the correlation of peaks to specific chemical compounds. Following a 12 h  $80$   $^{\circ}\text{C}$  drying period, capsules were placed in methylene chloride. The mixture of methylene chloride and capsules was sealed and allowed to stand for 1 week in order to allow the DCPD sufficient time to diffuse from the capsules into the solvent. GC was then performed on the filtered solution and confirmed the presence of both the endo and exo isomers of DCPD that were expected to be present in distilled DCPD [28]. Fig. 8 contains representative data corresponding to methylene chloride, endo-DCPD, and exo-DCPD for the  $180$   $\mu\text{m}$  capsules (Fig. 8a) compared to  $1.5$   $\mu\text{m}$  diameter capsules (Fig. 8b).

As in previous work, CHN data was used to estimate the DCPD and UF content of the capsules [25,29]. The carbon, hydrogen, and nitrogen content of the sonicated capsules was measured by combustion of a sample of prepared capsules, and analysis of the products (Exeter Analytical CE440). Since the UF shell wall was the only compound in the sample containing nitrogen, the mass percent of the UF follows directly from the measured nitrogen mass percent ( $W_N$ ). The DCPD mass percent was then calculated from the UF mass percent and the measured carbon mass percent ( $W_C$ ) [29]:

$$\begin{aligned} W_{\text{UF}} &= 4.003 W_N, \\ W_{\text{DCPD}} &= 1.101 W_C - 0.5895 W_{\text{UF}}. \end{aligned} \quad (1)$$

From the CHN data and Eq. (1), the average microcapsule DCPD content by mass was 78.4%. To determine the percent of filled volume in the capsules, a simple sphere in sphere model was used to represent the core-shell morphology of the capsule. Based on measured values of shell wall

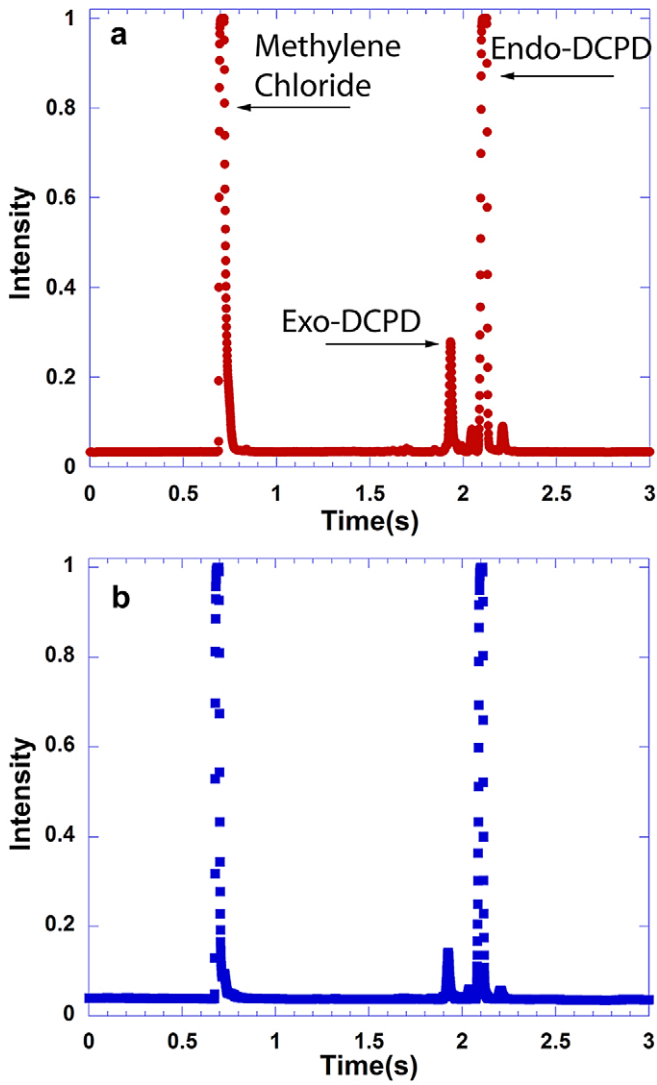


Fig. 8. Gas chromatograph of: (a) 180 μm mean diameter capsules (b) 1.5 μm mean diameter capsules prepared using sonication.

thickness, the mean capsule diameter, and the densities of DCPD (0.976 g/cm<sup>3</sup>) and UF (~1.15 g/cm<sup>3</sup>), the mean capsule fill percentage was estimated to be 94% by volume.

### 3.5. Capsule ζ-potential measurement

The ζ-potential of the capsules was studied to determine the ideal storage and processing pH for the capsules to avoid aggregation. Capsule solutions were prepared at pH levels ranging from 2 to 10 by dropwise addition of dilute aqueous sodium hydroxide and hydrochloric acid solutions. The samples were analyzed immediately after preparation to avoid agglomeration and sedimentation. The ζ-potential was measured by electrophoresis for each pH level (Malvern Zetasizer) as shown in Fig. 9. Each data point was the mean of at least 10 measurements from 2 independent batches. The isoelectric point (IEP) for the capsules was located at pH 2.2.

The encapsulation process described in Fig. 1a finishes with a pH of ~2.0 resulting in a low ζ-potential. Therefore,

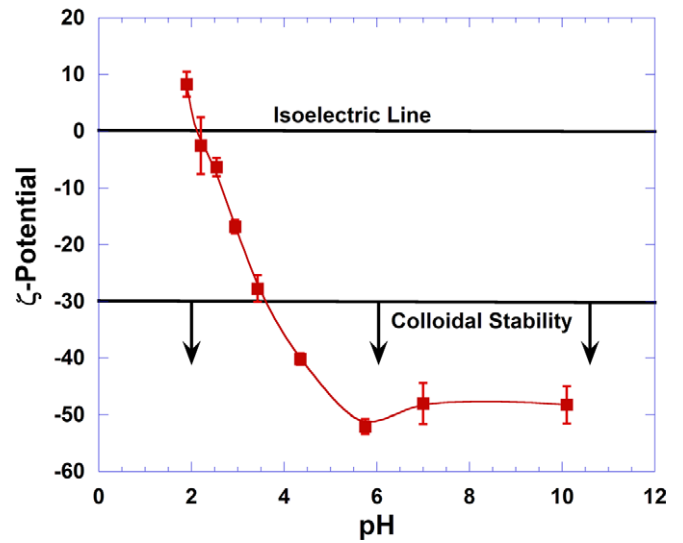


Fig. 9. ζ-Potential of 1.5 μm capsules measured by electrophoretic mobility.

it was necessary to raise the pH to prevent aggregation. In this study, particles with a higher ζ-potential (e.g. |ζ| > 30 mV) were considered electrostatically stable [30]. Agglomeration was minimized by raising the pH to a value between 3.5 and 4.0 with the addition of sodium hydroxide before storing the capsules or dispersing them in a polymer matrix. Higher pH values were not used because high alkalinity degraded the capsule shell walls over long periods of time.

## 4. Mechanical properties of epoxy/capsule composite

### 4.1. Elastic modulus and tensile strength

Measurements of the elastic modulus were obtained by dynamic mechanical analysis (DMA). The elastic modulus

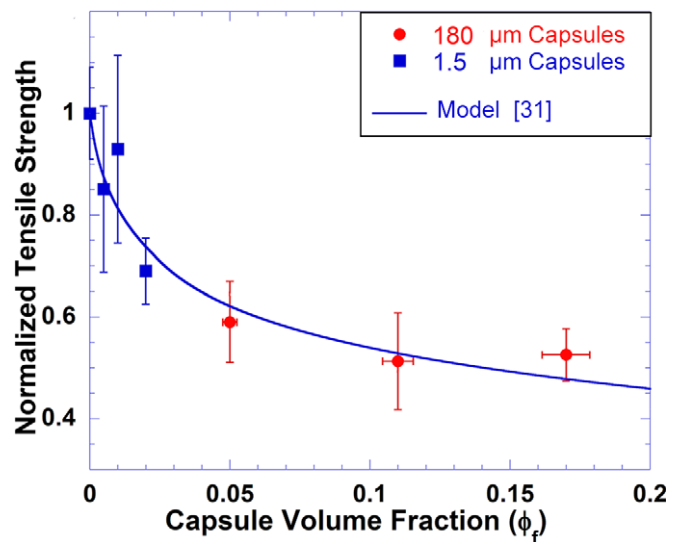


Fig. 10. Tensile strength of epoxy/capsule composite for large diameter capsules (●) [25], and smaller diameter capsules (■) is compared to the best fit Sudduth model [31].

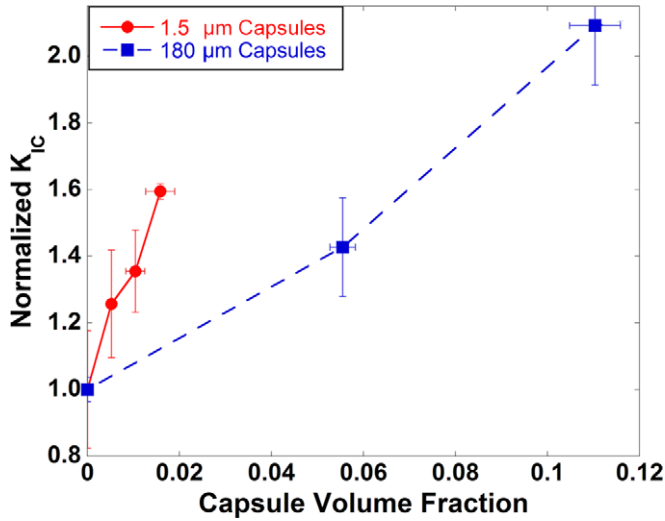


Fig. 11. Fracture toughness of epoxy/capsule composite with 1.5  $\mu\text{m}$  capsules (●) compared to data gathered previously by Brown et al. using 180  $\mu\text{m}$  capsules (■) [24].

Table 2  
Epoxy/capsule composite characterization

Volume fraction ( $\phi_f$ )	$E$ (GPa) <sup>a</sup>	$\sigma_c$ (MPa)	$K_{IC}$ (MPa $\text{m}^{1/2}$ )
0 – Virgin material	$2.88 \pm 0.27$	$37.9 \pm 3.4$	$0.95 \pm 0.18$
0.005	–	–	$1.20 \pm 0.15$
0.01	$2.91 \pm 0.13$	$31.9 \pm 4.74$	$1.29 \pm 0.16$
0.02	$2.90 \pm 0.17$	$26.2 \pm 2.45$	$1.52 \pm 0.02$

<sup>a</sup> DMA measurement of elastic modulus at 25 °C.

of the capsule filled composite was measured and compared between various capsule sizes and capsule volume fractions. Only a negligible change in modulus from the neat resin was observed with the addition of 0.5–2.0% volume fraction of the 1.5  $\mu\text{m}$  capsules. In contrast, Rzeszutko et al. [26] reported a proportional decrease in elastic modulus with increasing volume fraction of 180  $\mu\text{m}$  diameter capsules.

The ultimate tensile strength of epoxy with 1.5  $\mu\text{m}$  capsules at various concentrations was measured using the

sample shown in Fig. 2b and loaded to failure at a rate of 1 mm/min. As shown in Fig. 10, a drop in tensile strength was observed for capsule loadings up to  $\phi_f = 0.02$ . For comparison, the data from previous investigations of 180  $\mu\text{m}$  capsules is also plotted in Fig. 10 [26]. The decrease in tensile strength ( $\sigma_c$ ) for both capsule diameters was consistent with empirical models proposed by Sudduth for particulate composites [31]:

$$\frac{\sigma_c}{\sigma_o} = \left( \frac{\phi_{FZL} - \phi_f}{\phi_{FZL} + A\phi_f} \right)^\lambda \exp \left[ B\phi_{FZL} \left\{ 1 - \left( \frac{\phi_{FZL} - \phi_f}{\phi_{FZL}} \right)^\lambda \right\} \right]. \quad (2)$$

In Eq. (2),  $\sigma_o$  is the tensile strength of the neat resin; A, B, and the interaction coefficient ( $\lambda$ ) are fitting parameters; and the zero limit packing fraction ( $\phi_{FZL}$ ) is assumed to be the upper zero limit packing fraction ( $\phi_{FUZL} = 0.768$ ) given by Sudduth.

The dependence of tensile strength on average filler particle diameter has been studied by Landon et al. for a cross-linked polyurethane composite [32]. Their studies suggest that smaller particles have less of an effect on the tensile strength. While no significant change in tensile behavior was seen for 1.5  $\mu\text{m}$  capsules compared to 180  $\mu\text{m}$  capsules in our study, the tensile properties may be improved as we scale down further.

#### 4.2. Fracture toughness

The mode-I fracture toughness ( $K_{IC}$ ) of the epoxy/capsule composite was investigated over a range of capsule concentrations. As shown in Fig. 11,  $K_{IC}$  increased significantly with capsule volume fraction ( $\phi_f$ ). A 59% increase in fracture toughness was achieved for  $\phi_f = 0.015$ . The current data for sonicated capsules (ca. 1.5  $\mu\text{m}$  diameter) were also compared to data taken by Brown et al. for larger capsules (ca. 180  $\mu\text{m}$  diameter) [2]. As shown in Fig. 11, the increase in fracture toughness per volume fraction of capsules was substantially higher for 1.5  $\mu\text{m}$  capsules than for larger capsules. Further composite characterization details are summarized in Table 2.

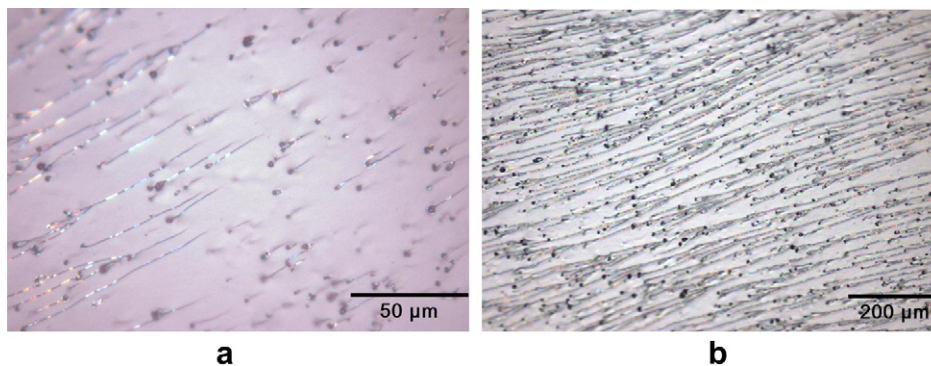


Fig. 12. Optical micrographs of the fracture surface of epoxy filled with well-dispersed 1.5  $\mu\text{m}$  capsules. Crack propagation is from left to right in these images.

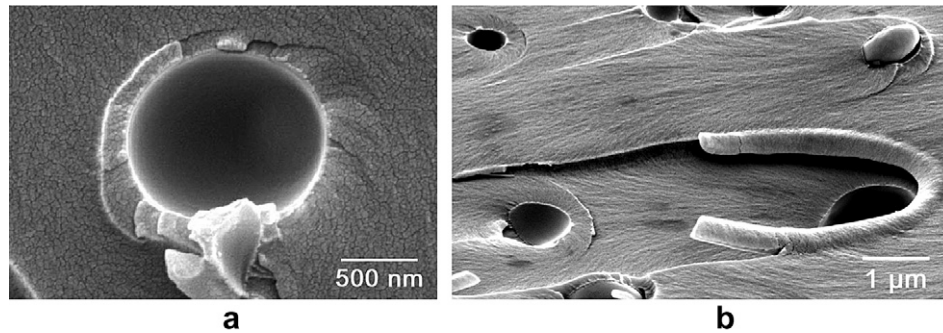


Fig. 13. (a) Top view of cleaved capsule embedded in epoxy with the shell wall exposed and crack tail extending toward the bottom of the micrograph and (b) three-dimensional crack tail structure on the fracture surface of epoxy/capsule composite. Crack propagation is from right to left in this image.

The fracture surfaces associated with well dispersed  $1.5\ \mu\text{m}$  capsules (Fig. 12) contained tail structures consistent with increased fracture toughness. Near the crack tip, tail structures extended a mean length of  $86\ \mu\text{m}$  ( $n = 130$ ) along the fracture surface. The tails associated with larger capsules ( $180\ \mu\text{m}$  diameter) extended an average of  $128\ \mu\text{m}$  ( $n = 60$ ). Hence, the ratio of tail length to diameter was significant for  $1.5\ \mu\text{m}$  capsules. Individual capsule rupture is evident in Fig. 13a. A tilted view of the fracture surface (Fig. 13b) reveals characteristic crack tail behavior indicative of crack deflection reported in previous nanoparticle fracture studies [24,33]. The crack deflection caused by the capsules was a key mechanism for the increased fracture toughness of the composite.

## 5. Conclusions

Healing agent-filled capsules with mean diameters as small as  $220\ \text{nm}$  and as large as  $1.65\ \mu\text{m}$  were prepared using an *in situ* UF encapsulation sonication technique. The prepared capsules had a smooth outer surface as opposed to the rough, debris covered UF capsules prepared by mechanical agitation. The capsule fill content was approximately 94% and they remained thermally stable to  $150\ ^\circ\text{C}$ , just below the boiling point of DCPD.

The capsules were successfully dispersed in an epoxy matrix up to  $\phi_f = 0.02$ . A slight decrease in the elastic modulus along with a more significant decrease in ultimate tensile strength was measured for composites with included capsules with a mean diameter of  $1.5\ \mu\text{m}$ . The decrease in tensile strength was accompanied by a significant increase in fracture toughness. Epoxy with dispersed sonicated capsules showed a nearly 59% increase in fracture toughness for a capsule volume fraction of  $\phi_f = 0.015$ . Fracture surfaces revealed that nearly all of the capsules ruptured during fracture. Significant crack tail formation on the fracture plane indicated active crack pinning and crack deflection mechanisms for increasing the fracture toughness of the composite.

The sonication process described in this study provides an efficient method for the production of nanocapsules that meet the requirements for self-healing materials. These smaller capsules will make self-healing materials responsive

to damage initiated at a scale that is not currently possible and compatible with composites where the reinforcement spacing requires smaller capsules for applications such as self-healing thin films, coatings, and adhesives.

## Acknowledgements

The authors would like to acknowledge the funding provided by the National Science Foundation through NanoCEMMS (NSF DMI 03-28162 COOP) and the Air Force Office of Scientific Research (FA9550-06-1-0553). The authors would also like to acknowledge Prof. Paul Braun and Aaron Jackson for providing the TEM images of the nanocapsules as well as the work of the autonomic materials group, and in particular Nathan Bosscher for preliminary work, Byron McCaughey, Joe Rule, Gerald Wilson, Michael Keller, David McIlroy, Alyssa Rzesutko, and Jessica Berry.

## References

- [1] White SR, Sottos NR, Geubelle PH, Moore JS, Kessler MR, Sriram SR, et al. Autonomic healing of polymer composites. *Nature* 2001;409(6822):794–7.
- [2] Brown EN, Sottos NR, White SR. Fracture testing of a self-healing polymer composite. *Exp Mech* 2002;42(4):372–9.
- [3] Brown EN, White SR, Sottos NR. Retardation and repair of fatigue cracks in a microcapsule toughened epoxy composite – Part II: In situ self-healing. *Comp Sci Tech* 2005;65(15-16):2474–80.
- [4] Kessler MR, Sottos NR, White SR. Self-healing structural composite materials. *Compos Part A Appl Sci Manuf* 2003;34(8):743–53.
- [5] Brown EN, Kessler MR, Sottos NR, White SR. In situ poly(urea-formaldehyde) microencapsulation of dicyclopentadiene. *J Microencapsul* 2003;20(6):719–30.
- [6] Ramírez LP, Landfester K. Magnetic polystyrene nanoparticles with a high magnetite content obtained by miniemulsion processes. *Macromol Chem Phys* 2003;204(1):22–31.
- [7] Ni PH, Zhang MZ, Yan NX. Effect of operating variables and monomers on the formation of polyurea microcapsules. *J Membrane Sci* 1995;103(1-2):51–5.
- [8] Zhang XX, Fan YF, Tao XM, Yick KL. Fabrication and properties of microcapsules and nanocapsules containing *n*-octadecane. *Mater Chem Phys* 2004;88(2-3):300–7.
- [9] Lansalot M, Davis TP, Heuts JPA. RAFT miniemulsion polymerization: Influence of the structure of the RAFT agent. *Macromolecules* 2002;35(20):7582–91.

- [10] Tiarks F, Landfester K, Antonietti M. Preparation of polymeric nanocapsules by miniemulsion polymerization. *Langmuir* 2001;17(3):908–18.
- [11] Alexandridou S, Kiparissides C, Mange F, Foissy A. Surface characterization of oil-containing polyterephthalamide microcapsules prepared by interfacial polymerization. *J Microencapsul* 2001;18(6):767–81.
- [12] Asua JM. Miniemulsion polymerization. *Prog Polym Sci* 2002;27(7):1283–346.
- [13] Schork FJ, Luo YW, Smulders W, Russum JP, Butte A, Fontenot K. Miniemulsion Polymerization. In: Okubo M, editor. *Polymer Particles*, vol. 175. Berlin/Heidelberg: Springer; 2005.
- [14] Anderson TL. *Fracture mechanics: fundamentals and applications*. 2nd ed. CRC Press; 1995.
- [15] Lee J, Yee AF. Inorganic particle toughening I: micro-mechanical deformations in the fracture of glass bead filled epoxies. *Polymer* 2001;42(2):577–88.
- [16] Tvergaard V. Effect of ductile particle debonding during crack bridging in ceramics. *Int J Mech Sci* 1992;34(8):635–49.
- [17] Faber KT, Evans AG. Crack deflection processes. II Experiment. *Acta Metall* 1983;31(4):577–84.
- [18] Kinloch AJ, Taylor AC. The mechanical properties and fracture behaviour of epoxy-inorganic micro- and nano-composites. *J Mater Sci* 2006;41(11):3271–97.
- [19] Cardoso RJ, Shukla A, Bose A. Effect of particle size and surface treatment on constitutive properties of polyester-cenosphere composites. *J Mater Sci* 2002;37(3):603–13.
- [20] Kinloch AJ, Mohammed RD, Taylor AC, Eger C, Sprenger S, Egan D. The effect of silica nano particles and rubber particles on the toughness of multiphase thermosetting epoxy polymers. *J Mater Sci* 2005;40(18):5083–6.
- [21] Rosso P, Ye L, Friedrich K, Sprenger S. A toughened epoxy resin by silica nanoparticle reinforcement. *J Appl Polym Sci* 2006;100(3):1849–55.
- [22] Day RJ, Lovell PA, Dorian P. Toughening of epoxy resins using particles prepared by emulsion polymerization: effects of particle surface functionality, size and morphology on impact fracture properties. *Polym Int* 1997;44(3):288–99.
- [23] Naous W, Xiao-Yan Y, Qing-Xin Z, Naito K, Kagawa Y. Morphology, tensile properties, and fracture toughness of epoxy/ $\text{Al}_2\text{O}_3$  nanocomposites. *J Polym Sci Polym Phys* 2006;44(10):1466–73.
- [24] Brown EN, White SR, Sottos NR. Microcapsule induced toughening in a self-healing polymer composite. *J Mater Sci* 2004;39(5):1703–10.
- [25] Brown EN. Fracture and fatigue of a self-healing polymer composite material. PhD Thesis, University of Illinois at Urbana-Champaign, Department of Theoretical and Applied Mechanics, 2003.
- [26] Rzesutko AA, Brown EN, Sottos NR. Tensile properties of self-healing epoxy. TAM Tech Rep 2003:1041–55.
- [27] Rule JD, White SR, Sottos NR. Effect of microcapsule and crack sizes on the performance of self-healing materials. *Polymer* 2007;48(12):3520–9.
- [28] Rule JD, Moore JS. ROMP reactivity of endo- and exo-dicyclopentadiene. *Macromolecules* 2002;35(21):7878–82.
- [29] Kessler MR. Characterization and performance of a self-healing composite material. Ph.D Thesis, University of Illinois at Urbana-Champaign, Theoretical and Applied Mechanics, 2002.
- [30] Hunter RJ. *Zeta potential in colloid science*. Academic Press; 1981.
- [31] Sudduth RD. Analysis of the maximum tensile strength of a composite with spherical particulates. *J Compos Mater* 2006;40(4):301–31.
- [32] Landon G, Lewis G, Boden GF. The influence of particle size on the tensile strength of particulate-filled polymers. *J Mater Sci* 1977;12(8):1605–13.
- [33] Kitey R, Tippur HV. Role of particle size and filler-matrix adhesion on dynamic fracture of glass-filled epoxy. II. Linkage between macro- and micro-measurements. *Acta Mater* 2005;53(4):1167–78.